Nuclear Physics B328 (1989) 36–58
North-Holland, Amsterdam

HYPERON PRODUCTION AT 200 AND 900 GeV C.M. ENERGY

UA5 Collaboration

R.E. ANSORGE[3], B. ÅSMAN[5], L. BUROW[1], P. CARLSON[5,a], R.S. DeWOLF[3], B. ECKART[1,b], G. EKSPONG[5], C. FUGLESANG[5,c], J. GAUDAEN[2,d], C. GEICH-GIMBEL[1], B. HOLL[1], R. HOSPES[1], K. JON-AND[5], F. LOTSE[5], N. MANTHOS[4,e], D.J. MUNDAY[3], J.E.V. OVENS[3], W. PELZER[1], J.G. RUSHBROOKE[3], F. TRIANTIS[4,e], L. VAN HAMME[2], C. WALCK[5], C.P. WARD[3], D.R. WARD[3], C.J.S. WEBBER[3], T.O. WHITE[3], G. WILQUET[2] and N. YAMDAGNI[5]

[1] *Physikalisches Institut der Universität Bonn, D-5300 Bonn, FRG*
[2] *Inter-University Institute for High Energies (ULB-VUB), B-1050 Brussels, Belgium*
[3] *Cavendish Laboratory of Physics, University of Cambridge, Cambridge CB3 OHE, UK*
[4] *CERN, CH-1211 Geneva 23, Switzerland*
[5] *Institute of Physics, University of Stockholm, S-113 46 Stockholm, Sweden*

Received 10 April 1989

The production of Λ's and Ξ^-'s in proton–antiproton collisions at 200 and 900 GeV c.m. energy has been studied using decays observed in the UA5 streamer chambers. The results are compared to previously published 546 GeV data, to results from other experiments, and to four theoretical models. The Λ yield per inelastic event is estimated to be 0.42 ± 0.11 at 200 GeV and 0.66 ± 0.14 at 900 GeV. We find a mean number of Ξ^-'s per inelastic collision of $0.03^{+0.04}_{-0.02}$ at 200 GeV and $0.06^{+0.05}_{-0.03}$ at 900 GeV. The average transverse momentum of Λ's in the rapidity region $|y| \leqslant 2$ is found to be $0.80^{+0.20}_{-0.14}$ GeV/c at 200 GeV and 0.74 ± 0.09 GeV/c at 900 GeV. The average transverse momentum of Ξ^-'s in the rapidity region $|y| \leqslant 3$ is estimated to be $0.8^{+0.4}_{-0.2}$ GeV/c at 200 GeV and $0.7^{+0.2}_{-0.1}$ GeV/c at 900 GeV which is lower than the unexpectedly high value of 1.1 ± 0.2 GeV/c measured at 546 GeV. The ratio of Ξ^- production to Λ production in the region $|y| \leqslant 2$, $p_t > 1$ GeV/c is $0.07^{+0.08}_{-0.04}$ at 900 GeV. This value is consistent with the ratio found in e^+e^- collisions and lower energy pp collisions but lower than the value obtained at 546 GeV. The average particle composition of events at 200 and 900 GeV, estimated using UA5 data, is presented.

1. Introduction

A high-energy hadronic collision is a complicated process involving many steps leading to the production of many particles. Quantum chromodynamics (QCD) is believed to be the correct theory for hadronic interactions, but for low momentum

[a] Now at the Manne Siegbahn Institute, S-104 05 Stockholm, Sweden.
[b] Now at INFN, Napoli, Italy.
[c] Now at CERN.
[d] Also at the Universitaire Instellingen Antwerpen, Belgium.
[e] Also at the University of Ioannina, Ioannina, Greece.

0550-3213/89/$03.50

transfer processes its use is severely limited by computational problems. In recent years phenomenological models of hadronic collisions have therefore appeared. Some of them attempt to describe in detail the wealth of new minimum bias data coming from the CERN $\bar{p}p$ Collider. Most of these data are on light mesons (pions, kaons). Knowledge about the production of heavier particles and baryons is also needed to test fully the ideas underlying these models. In addition, heavy particles have the advantage that they "remember" more of the primary partonic interaction due to the nature of the fragmentation process and decay kinematics. Besides teaching us something about standard physics, hyperon production could signal new phenomena. For example, it is believed that enhanced hyperon production could be a sign of quark–gluon plasma formation [1].

The UA5 collaboration has previously published results on Λ and Ξ^- production* at 546 GeV c.m. energy [2,3]. The measured mean transverse momentum of Ξ^-'s was surprisingly large. Also the value found for the ratio of the Ξ^- yield to the Λ yield was unexpectedly high. In 1985 we again took data, this time at 200 and 900 GeV, the higher energy having been made possible by running the Collider in pulsed mode [4]. The experimental methods used are essentially the same at all three energies.

This paper is structured in the following way. In sect. 2, the experimental methods are explained, including descriptions of the detector and the scanning, correction, and fitting procedure. The physics results are presented in sect. 3. Finally, sect. 4 contains a comparison of our results with four particle production models.

2. Experimental procedures

2.1. DETECTOR AND DATA TAKING

The main components of the UA5 detector are two large (6 m × 1.25 m × 0.5 m) streamer chambers placed about 5 cm above and below the collision point, each viewed by three cameras. The chambers cover the solid angle where the great majority of particles are produced: ±5 units of pseudorapidity** and 95% of the azimuthal angle. The trigger was provided by two scintillator hodoscopes placed at the ends of the streamer chambers. A detailed description of the detector can be found in ref. [3]. We require the decay vertices of the hyperons to be inside the streamer chambers. A typical vertical component of the path length is 4.9 cm for Λ's and 2.6 cm for Ξ^-'s ($\langle p_t \rangle = 0.7$ GeV/c) which means that a useful fraction of the decays is seen. Decays occurring inside the chambers can be identified with high confidence due to the excellent two-track resolution of the order of 1 mm. The

* Unless otherwise stated we use the shorthand notation Λ for $\Lambda + \bar{\Lambda} + \Sigma^0 + \overline{\Sigma^0}$, Ξ for $\Xi^- + \overline{\Xi^-}$, and Ξ^0 for $\Xi^0 + \overline{\Xi^0}$.

** Pseudorapidity η is defined as $\eta = -\ln\tan(\theta/2)$, where θ is the c.m. production angle.

measuring and three-dimensional reconstruction procedure is described in ref. [3]. For the hyperon analysis we have used a sample of events taken with our non-single-diffractive (NSD) trigger which has an estimated efficiency of about 95% for NSD events while keeping the background down to approximately 5% (beam-gas interactions and single-diffractive events, for details see refs. [3,5,6]). The detector was essentially the same during the pulsed Collider run as during the earlier 546 GeV run.

2.2. IDENTIFICATION OF HYPERONS

2.2.1. Scanning. The decay channel used in the Λ analysis is $\Lambda \rightarrow p\pi^-$ which has a branching ratio of 64.2%. The signature looked for is a V pointing to the main vertex. In the Ξ^- analysis the decay mode $\Xi^- \rightarrow \Lambda\pi^-$, with a branching ratio of 100%, and $\Lambda \rightarrow p\pi^-$ was used. The topology is that of a primary track which undergoes a sharp change of direction (called a kink) and a V pointing to the kink vertex. Due to the short decay path of these particles the decays are clustered near the base of the streamer chambers. To avoid background due to random association of tracks and interactions just outside the visible volume the decay vertex was required to be inside the chamber.

The event samples consist of two classes of events which were treated differently with respect to the scanning and measurement procedure. The first class, called the normal sample, had been measured completely before being scanned for strange particles whereas events in the second class, called the special sample, were scanned first and subsequently fully measured if they contained a Ξ^- candidate. In events from the special sample containing a Λ candidate, in addition to the V tracks, five primary tracks were measured to allow the determination of the position of the primary interaction. For further details see ref. [7]. The number of events in the different classes is given in table 1.

TABLE 1
The number of NSD events scanned for Λ's and Ξ^-'s. The different classes of events are explained in the text.

c.m. energy (GeV)	Event sample	Λ	Ξ^-
200	normal	3480	3480
	special	598	3664
	total	4078	7144
900	normal	5823	5823
	special	980	5395
	total	6803	11218

In addition to being scanned, the normal sample measurements were searched for V's and kinks by a computer program. The search criteria were loose versions of the final cuts described below. The program did not attempt to find Ξ^- candidates by coupling together associated kinks and V's. This was left to the check scan (see below). Since a software search was impossible for the special sample it was replaced by a second, independent, visual scan.

Each candidate was inspected on the scanning table by a physicist to check that it fulfilled the criteria of the visual scan. Many software search candidates could be dismissed as random associations of tracks which contaminated the sample due to the rather loose cuts. Each combination of a kink and a V occurring in the same frame was inspected to see if it constituted a Ξ^- candidate. Candidates with badly measured tracks were remeasured.

From the two independent scans we estimate the total scanning efficiency for Λ's and Ξ^-'s to be 98% at both energies.

TABLE 2
Criteria to be fulfilled to be accepted as a hyperon candidate

Cuts applied to Λ candidates	
Length of each track	$\geqslant 15$ cm
Track fit RMS	$\leqslant 30$ μm
Opening angle	$\geqslant 8°$
Coplanarity cut	$d \leqslant 4 - \delta$
Distance between decay vertex and entrance plane of visible volume	$\geqslant 0.5$ cm
Straddling	yes
Distance between decay vertex and beam axis	$\leqslant 40$ cm
$\lvert\cos\theta_K^*\rvert$	$\geqslant 0.5$
Abs. value of rapidity	$\leqslant 2$
Cuts applied to Ξ^- candidates	
Length of each V track	$\geqslant 15$ cm
Track fit RMS	$\leqslant 30$ μm
Opening angle of kink	$\geqslant 3°$
Opening angle of V	$\geqslant 3°$
V coplanarity cut	$d \leqslant 4 - \delta$
Distance between decay vertex and entrance plane of visible volume	$\geqslant 3$ cm
Distance between kink vertex and V vertex	$\geqslant 3$ cm
V straddling	yes
Abs. value of rapidity	$\leqslant 3$

The variable d is the distance in cm between the primary interaction point and the plane formed by the V tracks and δ is the angle in degrees between this plane and the flight path of the decaying particle. The variable θ_K^* is the c.m. decay angle of the Λ candidate when analyzed as a K_S^0. The rapidity of a particle with energy E and longitudinal moment p_ℓ is defined as $y = \frac{1}{2}\ln[(E + p_\ell)/(E - p_\ell)]$.

TABLE 3
The observed number of Λ and Ξ^- decays

c.m. energy (GeV)	p_t range (GeV/c)	Λ $\lvert y\rvert \leqslant 2$	Ξ^- $\lvert y\rvert \leqslant 2$	Ξ^- $\lvert y\rvert \leqslant 3$
200	all p_t	168	3	3
	> 0.5	139	3	3
	> 1	63	3	3
900	all p_t	463	6	7
	> 0.5	379	6	7
	> 1	172	4	5

2.2.2. The final sample. Several cuts were applied to the candidates found in the scanning in order to minimize the background, to allow an accurate calculation of the dynamical quantities, and to ensure a high and uniform scanning efficiency. The cuts are listed in table 2. The opening angle cut of 8° for Λ's was increased from the value of 3° used in our 546 GeV Λ analysis [3] and in our K^0_S analysis [7]. This was done in order to improve the precision of the momentum determination which is worse for Λ's as compared to K^0_S's for equal opening angles due to the decay geometry [8]. For a more detailed discussion of the cuts see refs. [3, 9].

All criteria in table 2 except the rapidity and $\cos\theta^*_K$ criteria are purely geometrical. The UA5 detector has no magnetic field for the measurement of particle momenta. However, the momenta of particles in the decay topologies studied can be calculated from the track angles, once a hypothesis about the identities of the particles is made. A kinematical, least squares fit was made to the decay hypothesis taking into account the measurement errors and correlations of the track parameters [8]. There are two possibilities when assigning masses to the V tracks. However, the hypothesis giving the lower Λ or Ξ^- momentum can always be rejected since it corresponds to a negligible probability for the particle to reach the chamber. Monte Carlo simulations show that the precision in the transverse momentum determination is about 5% for both Λ's and Ξ^-'s.

The sizes of the final Λ and Ξ^- samples in different regions of phase space are given in table 3.

2.3. CORRECTION OF DATA

2.3.1. Background subtraction. The K^0_S background in the Λ sample is shown for the variable $|\cos\theta^*_K|$ in fig. 1. About half of the K^0_S background is eliminated by requiring that $|\cos\theta^*_K| \geqslant 0.5$, since the distribution for observed K^0_S is approximately flat. Only about 3% of the primary Λ's are lost by this cut. This is due to the fact that Λ decays tend to be asymmetric in the lab frame (the heavier proton tends

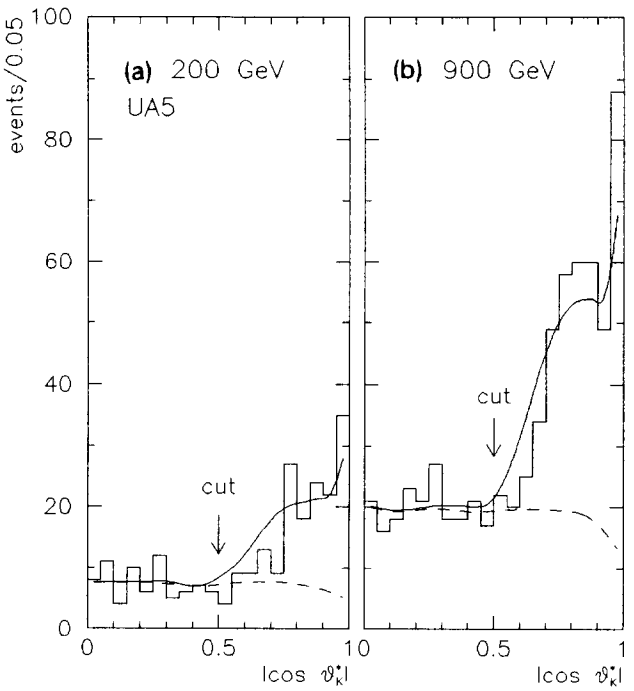

Fig. 1. The $|\cos\theta_K^*|$ distribution of V's passing the Λ cuts at (a) 200 GeV and (b) 900 GeV. The solid line is the expected distribution calculated using the measured Λ and Ξ^- rates and a kaon rate adjusted to give the correct number of observed candidates in the region $|\cos\theta_K^*| < 0.5$. The dashed line shows the expected kaon contribution. The $|\cos\theta_K^*|$ cut is indicated with the arrow.

to be emitted more forward than the pion). When interpreted as K_S^0 decays and boosted to the kaon rest frame they obtain large values of $|\cos\theta_K^*|$. The remaining background is expected to be Λ from Ξ^-/Ξ^0 decays and K_L^0. The background from photon conversion is estimated to be less than 0.1% at both energies. The estimated sizes of the background sources are given in table 4. It is clear from table 4 that the main source of background in the Λ sample is K_S^0 decay. The background was estimated using MC simulated events with UA5 data on K_S^0 [7], Ξ^- and charged particle [10] production used as input.

Two methods were used to subtract the K_S^0 background from the Λ sample. In the first, 0.5 is added to the $|\cos\theta_K^*|$ of the V's with $|\cos\theta_K^*| < 0.5$. The V's are then reanalyzed as Λ's and subtracted statistically from the Λ sample. This was the procedure used in the 546 GeV analysis [3,11]. In the second method the K_S^0 background is generated by a MC program and subtracted. The background was normalized to the observed number of coplanar V's with $|\cos\theta_K^*| < 0.5$. The results obtained using the two methods were consistent and in the following we will present their average.

TABLE 4
Contamination in the Λ sample in the region $p_t > 0.5$ GeV/c estimated using our measured K^0_S [7] and Ξ^- yields and a MC program. The K^0_S and K^0_L yields are assumed to be equal. The errors quoted are statistical only

Type of contamination	Contamination (%)	
	200 GeV	900 GeV
K^0_S	31 ± 5	35 ± 3
$\Xi^0 \to \Lambda$	7 ± 7	9 ± 3
$\Xi^- \to \Lambda$	7 ± 7	9 ± 3
K^0_L	0.3 ± 0.2	0.4 ± 0.2

The K^0_L background correction is very small and was incorporated in the factor, described below, which corrects for measurement errors and interactions of the particles with the material of the detector.

The background from $\Xi^- \to \Lambda\pi^-$ and $\Xi^0 \to \Lambda\pi^0$ decays was generated using a MC program. The Λ analysis was limited to $p_t > 0.5$ GeV/c to avoid the low p_t region where the relative size of the background is larger. The subtraction of Λ's from Ξ's introduces large errors since the p_t distribution and rate of the Ξ hyperons are poorly known (see sect. 3). The values of $\langle p_t \rangle_{\Xi^-}$ and $\langle n_{\Xi^-} \rangle$ found at 900 GeV are much lower than the values at 546 GeV, probably due to statistical fluctuations. We conclude that the best values to use for the background subtraction are those given by a fit to the combined 546 and 900 GeV data. This fit gave $\langle p_t \rangle_{\Xi^-} = 0.9 \pm 0.1$ GeV/c and $\langle n_{\Xi^-} \rangle = 0.06 \pm 0.02$ for all p_t in the region $|y| \leqslant 3$. The raw p_t distribution of the Λ sample is given in fig. 2 with the different background components shown separately.

The main sources of background to the Ξ^- sample are:

(i) $\pi^\pm$ and $K^\pm$ interacting in the streamer chamber (SC) gas giving one charged particle and a K^0_S or Λ.

(ii) Photons from $K^\pm \to \pi^\pm\pi^0$ and $\Sigma^+ \to p\pi^0$ decays which convert in the SC gas.

(iii) Random association of a V from the primary vertex to a kink vertex.

(iv) $\pi^\pm$ interacting in the SC gas giving one charged particle and a photon which converts in the gas.

In 34000 (29000) events generated at 200 (900) GeV with the UA5 MC program [12] no background event of the above types was found which gave a kinematic fit to the Ξ^- hypothesis. We conclude that the background in our Ξ^- sample is at most 0.6 (1) events at 200 (900) GeV (95% confidence level).

2.3.2. Correction and fitting procedure. The geometrical acceptance g was obtained by numerically integrating the distributions of the kinematical quantities over the domain defined by the geometrical cuts. Fig. 3 shows the Λ and Ξ^- acceptance

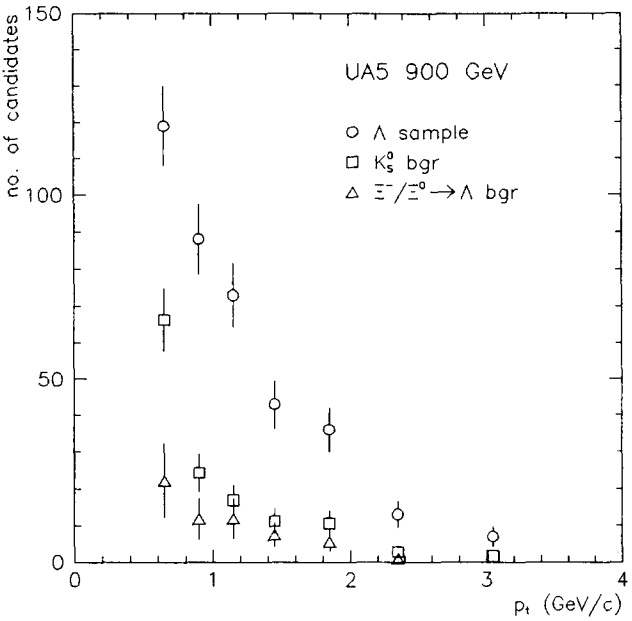

Fig. 2. The observed p_t distribution of Λ's at 900 GeV with the estimated background contributions from K^0_S and Λ's coming from Ξ^- and Ξ^0 decays shown. The 200 GeV distributions are similar.

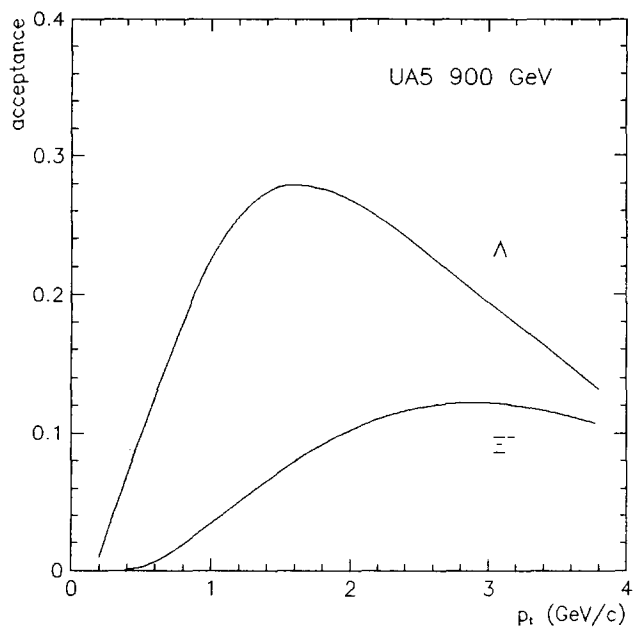

Fig. 3. The Λ and Ξ^- acceptances at 900 GeV as a function of p_t. The acceptances do not include branching ratios. The 200 GeV acceptances are very similar.

as a function of p_t. For Λ's we have made an additional correction for effects due to interactions, measurement errors, and contamination from K_L^0's. The overall acceptance, not including the branching ratios, is about 12% for the Λ's and 2% for the Ξ^-'s. The low acceptance is mainly due to the short hyperon lifetimes.

An exponential function in p_t was used to fit the corrected p_t distributions of the Λ's and Ξ^-'s:

$$\frac{d\sigma}{dp_t^2} \propto \exp(-2p_t/\langle p_t\rangle). \tag{1}$$

The Λ sample was fitted by the method of least squares. The mean number of Λ's per event was calculated by integrating the fitted p_t function over all p_t. The generalized maximum likelihood (ML) method was used to fit simultaneously the p_t function and the rate to the Ξ^- data. The fit parameters are $\langle p_t\rangle$, the average transverse momentum and $\langle n\rangle$, the corrected Ξ^- yield per event. The likelihood function employed was

$$\mathcal{L} = \frac{\mu^{n_{obs}} \exp(-\mu)}{n_{obs}!} \prod_{i=1}^{n_{obs}} f(p_{ti}),$$

$$f(p_{ti}) = \frac{g(p_{ti})\, p_{ti} \exp(-2p_{ti}/\langle p_t\rangle)}{\int_0^\infty g(p_t)\, p_t \exp(-2p_t/\langle p_t\rangle)\, dp_t},$$

$$\mu = \langle n\rangle NB \frac{\int_0^\infty g(p_t)\, p_t \exp(-2p_t/\langle p_t\rangle)\, dp_t}{\int_0^\infty p_t \exp(-2p_t/\langle p_t\rangle)\, dp_t}, \tag{2}$$

where n_{obs} is the number of observed Ξ^-'s, N is the number of events, and B is the branching ratio for the Ξ^- decay mode used. For the Ξ^-'s, the errors were found by the graphical method, i.e. using the extreme values of the 39% likelihood contour of $\mathcal{L}(\langle p_t\rangle, \langle n\rangle)$.

The above correction procedure is strictly correct only if two conditions are fulfilled: (i) the invariant cross section factorizes, $(1/\pi)\, d^2\sigma/dy\, dp_t^2 = f_1(p_t) f_2(y)$ and (ii) the rapidity distribution $f_2(y)$ used in the calculation of $g(p_t) = \int f_2(y) g(p_t, y)\, dy$ is correct. The factorization of the invariant cross section cannot be checked with the data itself due to the low statistics but is known to hold in the central region for our kaon data [7,9]. The choice of rapidity distribution is not critical in the limited regions of rapidity considered in this analysis. The acceptance $g(p_t)$ was calculated using the y distribution produced by the UA5 MC program. Also the extrapolation of the rates from the limited rapidity region to full phase space was done using this y distribution.

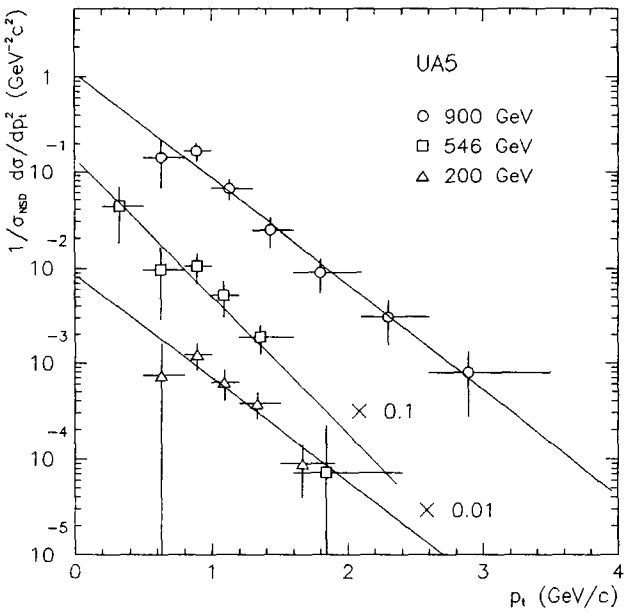

Fig. 4. The corrected p_t distributions of Λ's at 200, 546, and 900 GeV. The lines are exponential functions in p_t which have been fitted to the data. The 546 GeV data is from ref. [3].

3. Results and discussion

3.1. TRANSVERSE MOMENTA

The corrected p_t distribution of Λ's in the rapidity range $|y| \leqslant 2$ is shown in fig. 4. The data are seen to follow the exponential form within errors. We obtain an average transverse momentum of $0.80^{+0.20}_{-0.14}$ GeV/c at 200 GeV and 0.74 ± 0.09 GeV/c at 900 GeV.

The observed Ξ^- distributions at 900 GeV for different variables are given in fig. 5 together with curves obtained from MC simulation. The data and MC curves are seen to be consistent. This is also true for the smaller 200 GeV data sample not shown.

The observed Ξ^- transverse momentum distribution at 900 GeV in the region $|y| \leqslant 3$ is shown in fig. 5a. The MC curve was calculated using the fitted p_t function. The average transverse momentum resulting from the ML fit was $0.8^{+0.4}_{-0.2}$ GeV/c at 200 GeV and $0.7^{+0.2}_{-0.1}$ GeV/c at 900 GeV. These values are lower than our previously published result at 546 GeV, 1.1 ± 0.2 GeV/c [2, 3], but all three values are compatible within errors.

Our results are summarized and compared to our kaon results in table 5. The evolution of $\langle p_t \rangle$ with energy is shown in fig. 6. Our 546 GeV results as well as data for Λ's, protons, charged hadrons, and pions from other experiments are included

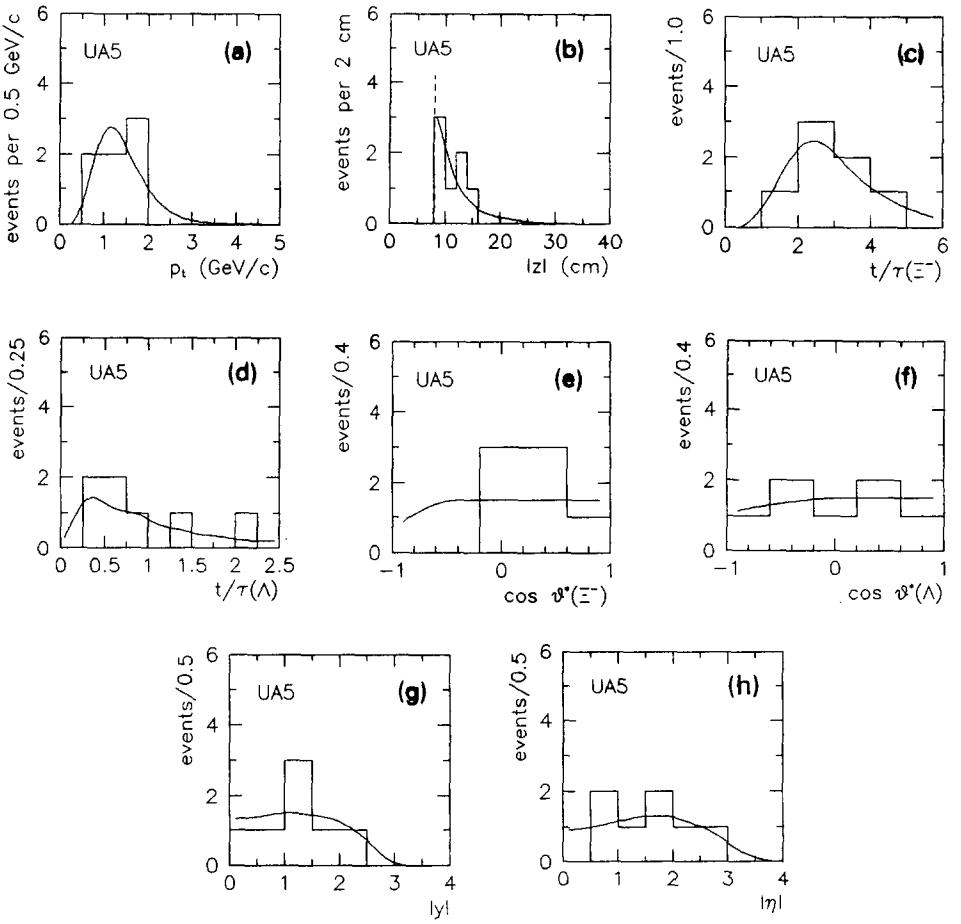

Fig. 5. Observed distributions of Ξ^-'s at 900 GeV. The curves are the expected distributions calculated using MC simulation and normalized to the number of observed Ξ^-'s. The variables plotted are (a) p_t, (b) $|z|$, the z coordinate of the Ξ^- decay vertex (the dashed line indicates the position of the z cut), (c) $t/\tau(\Xi^-)$, the proper time from the production point to the decay point of the Ξ^-, (d) $t/\tau(\Lambda)$, the proper time from the production point to the decay point of the Λ from the Ξ^- decay, (e) $\cos\theta^*(\Xi^-)$, the angle of the Λ in the Ξ^- rest frame, (f) $\cos\theta^*(\Lambda)$, the angle of the proton in the Λ rest frame, (g) $|y|$, and (h) $|\eta|$.

for comparison. The error on each antiproton and pion point below 200 GeV is assumed to be 5%. The 546 GeV pion and proton results have been estimated from fits [9] to UA2 data [15].

Knowing the transverse momentum distribution we can correct the lifetime distribution of primary Λ's and see if it has the correct shape and normalization, thereby cross-checking our analysis procedure. In fig. 7 the proper lifetime distribu-

TABLE 5
Average transverse momenta of strange particles as measured by the UA5 experiment at 200, 546 and 900 GeV c.m. energy [2, 3, 7, 9]. The notation Λ stands for $\Lambda + \bar{\Lambda} + \Sigma^0 + \bar{\Sigma}^0$ and Ξ^- signifies $\Xi^- + \bar{\Xi}^-$.

Particle	y region	$\langle p_t \rangle$ (GeV/c)		
		200 GeV	546 GeV	900 GeV
K^0_S	$\lvert y \rvert \leqslant 2.5$	$0.53^{+0.08}_{-0.06}$	0.57 ± 0.03	$0.62^{+0.09}_{-0.07}$
Λ	$\lvert y \rvert \leqslant 2$	$0.80^{+0.20}_{-0.14}$	0.62 ± 0.08	0.74 ± 0.09
Ξ	$\lvert y \rvert \leqslant 3$	$0.8^{+0.4}_{-0.2}$	1.1 ± 0.2	$0.7^{+0.2}_{-0.1}$

tion of primary Λ's is shown. It is seen to be consistent with the expected exponential function.

The observed proper lifetime distributions of the Ξ^-'s and their daughter Λ's at 900 GeV are given in fig. 5c, d. Fig. 5b shows the distribution of the Ξ^- decay vertex along the vertical axis perpendicular to the chamber base (z axis), at 900 GeV. The vertices are clustered near the base of the chamber as expected. The decay

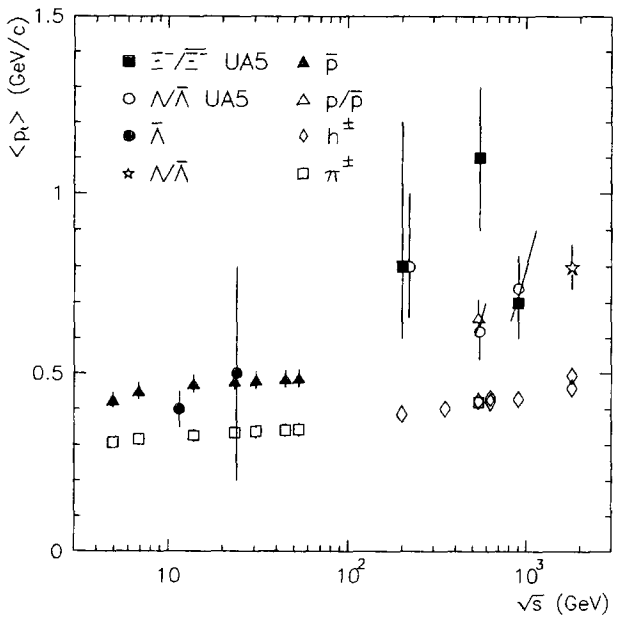

Fig. 6. The average transverse momentum of Λ's and Ξ^-'s plotted as a function of c.m. energy. Also shown are data from other experiments on Λ's [13], protons [14,15], charged hadrons [16], and pions [14,15].

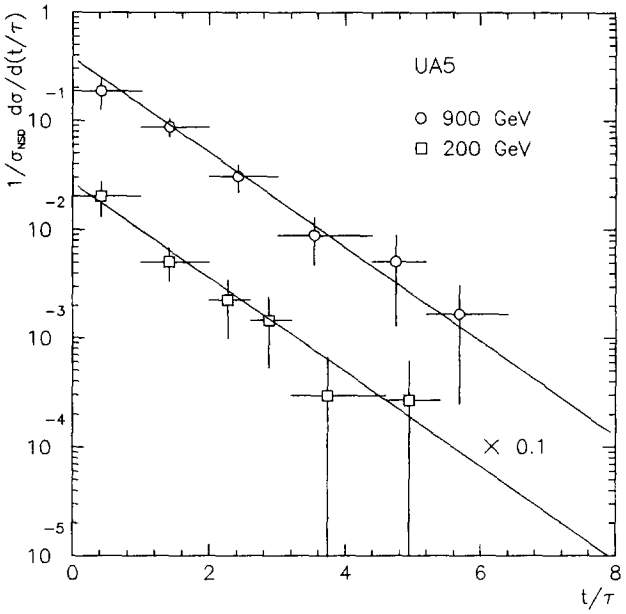

Fig. 7. The corrected proper lifetime distribution of Λ's at 200 and 900 GeV. The lines are exponential functions expected from the known lifetime and normalized to the Λ rate as determined from the p_t distributions.

angular distributions of Λ's and Ξ^-'s in their respective rest frames at 900 GeV are given in fig. 5e and 5f, respectively. The curves were calculated assuming flat $\cos\theta^*$ distributions.

3.2. HYPERON YIELDS

We consider the Ξ^- yield first since this result is used in the Λ background correction. The mean number of Ξ^-'s per NSD event in the region $|y| \leqslant 3$, $p_t > 1$ GeV/c, where we have reasonable detection efficiency (see fig. 3), was found to be $0.011^{+0.040}_{-0.008}$ at 200 GeV and $0.011^{+0.020}_{-0.007}$ at 900 GeV. The rate for all p_t was determined by fitting the exponential function to all data and extrapolating it to $p_t = 0$. We obtained $0.03^{+0.04}_{-0.02}$ at 200 GeV and $0.05^{+0.04}_{-0.02}$ at 900 GeV for all p_t, $|y| \leqslant 3$. Due to the acceptance the mean number of Ξ^-'s is highly negatively correlated with the average transverse momentum, which has a large error. The likelihood contours in fig. 8 illustrate this. If one fixes the average transverse momentum at 900 GeV to the 546 GeV value, for example, one gets a mean number of about 0.02, which is much lower than the 546 GeV value of 0.08. This difference in the Ξ^- yield between the 546 GeV and the 900 GeV measurements was studied statistically. The probability for the actual outcome (16 Ξ^-'s at 546 GeV and 7 Ξ^-'s at 900 GeV) or "worse" was calculated assuming the true yields and average

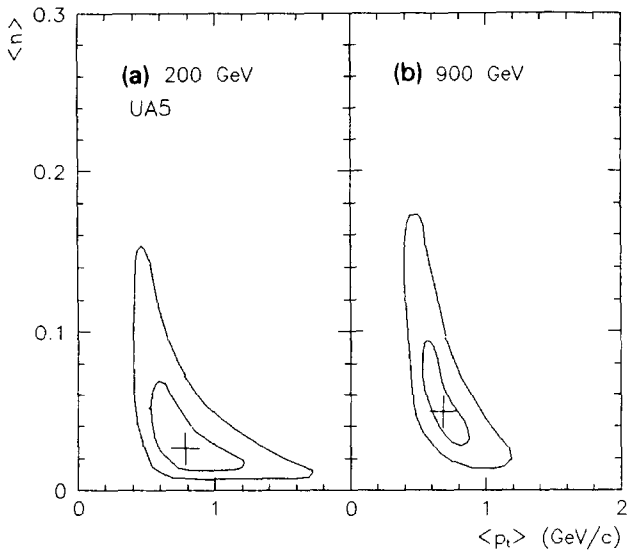

Fig. 8. Contour diagrams of the Ξ^- likelihood functions at (a) 200 GeV and (b) 900 GeV. The contours represent 39% and 86% joint likelihood regions for $\langle p_t \rangle$ and $\langle n \rangle$.

p_t's to be the same at the two energies. The probability thus obtained was 1% and the most probable outcome 9 (14) Ξ^-'s at 546 (900) GeV. Since the systematic uncertainties are almost identical at the two energies we conclude that the difference in observed rates is mainly due to statistical fluctuation. Using the UA5 MC program to extrapolate the Ξ^- yield from $|y| \leqslant 3$ to full phase space we obtain $0.03^{+0.04}_{-0.02}$ at 200 GeV and $0.07^{+0.06}_{-0.03}$ at 900 GeV. To allow comparisons with results from other experiments, these values have been extrapolated to mean numbers per *inelastic* event using the assumption that the Ξ^- to charged particle ratios are the same in single-diffractive and non-single-diffractive events. This assumption leads to the relation $\langle n_{\Xi^-} \rangle_{\text{inel}} = \langle n_{\Xi^-} \rangle_{\text{NSD}} R$, $R = \langle n_{\text{ch}} \rangle_{\text{inel}} / \langle n_{\text{ch}} \rangle_{\text{NSD}}$. The ratio R can be calculated using UA5 results on $\bar{\text{p}}\text{p}$ cross sections [5], single-diffraction [6], and charged multiplicities [10] and we obtain 0.907 ± 0.016 at 200 GeV and 0.872 ± 0.012 at 900 GeV. Using these ratios we calculate a Ξ^- yield per inelastic event of $0.03^{+0.04}_{-0.02}$ at 200 GeV and $0.06^{+0.05}_{-0.03}$ at 900 GeV.

We obtain a Λ yield per NSD event of 0.27 ± 0.07 at 200 GeV and 0.38 ± 0.08 at 900 GeV in the region $|y| \leqslant 2$. The dependence of $\langle p_t \rangle_\Lambda$ and $\langle n_\Lambda \rangle$ on the assumed value of $\langle p_t \rangle_{\Xi^-}$ is illustrated in fig. 9. The Ξ^- rate and average transverse momentum are negatively correlated. The fact that Λ's from Ξ^-/Ξ^0 are a source of background in the Λ sample leads to a positive correlation between the Λ yield and $\langle p_t \rangle_{\Xi^-}$. Since the background preferentially affects the higher transverse momenta, $\langle p_t \rangle_\Lambda$ is positively correlated with the Ξ^- yield and, in turn, negatively correlated with $\langle p_t \rangle_\Xi$. Extrapolating to all y we find a mean number of 0.46 ± 0.12 at 200

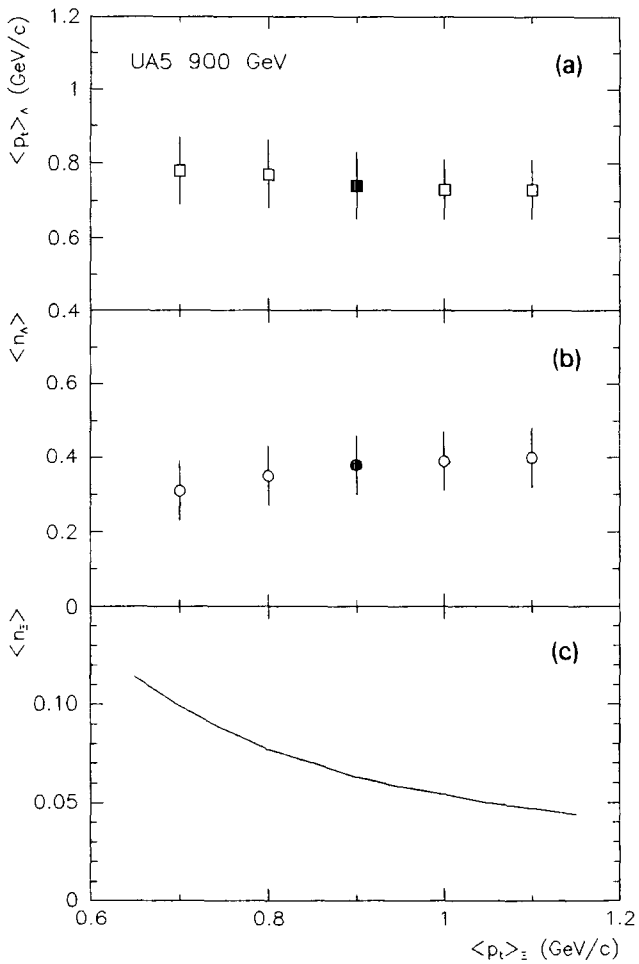

Fig. 9. The dependence of (a) $\langle p_t \rangle_\Lambda$, (b) $\langle n_\Lambda \rangle$ and (c) $\langle n_{\Xi^-} \rangle$ on the assumed value of $\langle p_t \rangle_{\Xi^-}$ at 900 GeV. The filled markers indicate the most probable values. $\langle n_{\Xi^-} \rangle$ and $\langle p_t \rangle_{\Xi^-}$ have been calculated using the combined 46 and 900 GeV sample. The results at 200 GeV are similar.

GeV and 0.76 ± 0.16 at 900 GeV. The yield per inelastic event is estimated at 0.42 ± 0.11 at 200 GeV and 0.66 ± 0.14 at 900 GeV.

The Λ and Ξ^- yields per inelastic event are plotted as a function of energy in fig. 10. UA5 data on antineutrons as well as data on $\bar{\Lambda}$'s and antiprotons from other experiments are shown for comparison. The curve is the result of a fit of a quadratic function in $\ln s$ to the $\Lambda/\bar{\Lambda}$ data:

$$\langle n_\Lambda \rangle_{\text{inel}} = (0.10 \pm 0.03) + (-0.039 \pm 0.010)\ln s + (0.0040 + 0.0008)\ln^2 s$$

(s expressed in GeV^2) with $\chi^2/\text{NDF} = 12/11$. This form has also been used in our

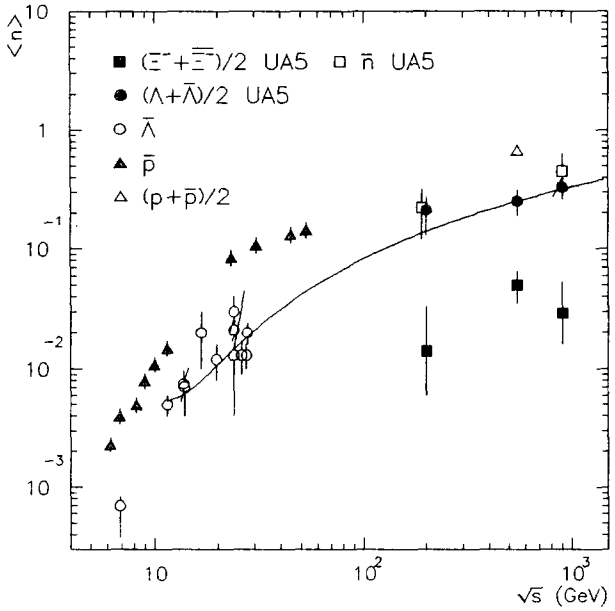

Fig. 10. The yields of Λ's and Ξ^-'s per inelastic event in pp ($\bar{p}p$) collisions as a function of c.m. energy. Data on antineutrons from this experiment [18] and data on $\bar{\Lambda}$'s [13,19,20] and protons [14,15] from other experiments are also shown. The 546 GeV proton yield has been established from a fit [9] to UA2 data [15]. Leading particles are excluded. The curve represents a fit of the function $\langle n_\Lambda \rangle_{\text{incl}} = a + b \ln s + c \ln^2 s$ to the Λ data above 10 GeV. The parameter values are given in the text.

TABLE 6

The average particle composition of non-single-diffractive events at 200, 546, and 900 GeV c.m. energy as measured by the UA5 experiment (for references see the text) or estimated using the assumptions in [3]. The leading particles, assumed to be one proton and one neutron per event on average, have been subtracted

Particle	$\langle n \rangle$		
	200 GeV	546 GeV	900 GeV
All charged	20.4 ±0.4	28.4 ±0.3	34.6 ±0.9
γ	22.2 ±2.4	33.0 ±3.0	41.4 ±4.1
$K^0 + \bar{K}^0$	1.50 ± 0.18	2.24 ± 0.16	2.74 ± 0.30
$K^+ + K^-$	1.50 ± 0.18	2.24 ± 0.16	2.74 ± 0.30
$n + \bar{n}$	0.5 ±0.2	1.45 ± 0.15	1.0 ±0.4
$p + \bar{p}$	0.5 ±0.2	1.45 ± 0.15	1.0 ±0.4
$\Lambda + \bar{\Lambda} + \Sigma^0 + \bar{\Sigma}^0$	0.46 ± 0.12	0.53 ± 0.11	0.76 ± 0.16
$\Sigma^+ + \bar{\Sigma}^+ + \Sigma^- + \bar{\Sigma}^-$	0.23 ± 0.06	0.27 ± 0.06	0.38 ± 0.08
$\Xi^- + \bar{\Xi}^-$	$0.03^{+0.04}_{-0.02}$	0.10 ± 0.03	$0.07^{+0.06}_{-0.03}$
$\Xi^0 + \bar{\Xi}^0$	$0.03^{+0.04}_{-0.02}$	0.10 ± 0.03	$0.07^{+0.06}_{-0.03}$
$e^+ e^-$	0.27 ± 0.03	0.41 ± 0.04	0.50 ± 0.05
$\pi^+ + \pi^-$	17.9 ±0.5	23.9 ±0.4	29.9 ±1.0

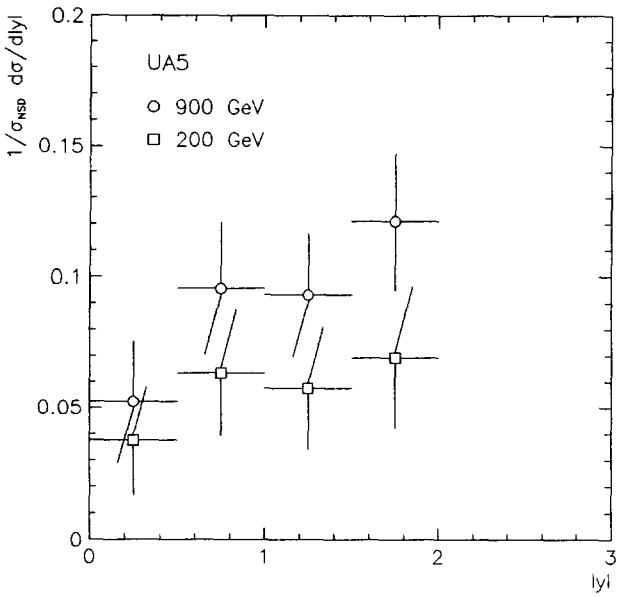

Fig. 11. The rapidity distribution of Λ's at 200 and 900 GeV.

charged particle multiplicity analysis [17]. It is suggested by the logarithmic rise in both the width and the height of the plateau of the charged particle pseudorapidity distribution [21].

In addition to Λ, Ξ^-, K^0_S [7,9], and antineutrons [3,18], UA5 has measured the yields of photons [3,22] and the total charged multiplicity [3,10]. Using the assumptions described in ref. [3] we can calculate the particle composition of an average NSD event at 200 and 900 GeV. The result is given in table 6 together with the earlier 546 GeV result [3].

3.3. RAPIDITY DISTRIBUTIONS

The rapidity distribution of Λ's is given in fig. 11. The distribution is fairly flat in the central region where we have acceptance. The observed rapidity and pseudorapidity distributions of Ξ^-'s at 900 GeV are shown in fig. 5g, h.

3.4. PARTICLE RATIOS

The ratio of Ξ^- production to Λ production was calculated in the region $|y| \leqslant 2$, $p_t > 1$ GeV/c where we have a relatively high acceptance for both particles. We obtain $0.07^{+0.08}_{-0.04}$ at 900 GeV. This value and the corresponding confidence interval is given in table 7. The experimental correlation between the Ξ^- and Λ rates has been taken into account in the calculation. Results from 546 GeV [3], from pp collisions at 63 GeV [23], and from e^+e^- collisions [24–26] are also shown for comparison.

TABLE 7
The Ξ^-/Λ ratio in the region $|y| \leq 2$, $p_t > 1$ GeV/c at 900 GeV c.m. energy

Experiment	c.m. energy (GeV)	Type of interaction	p_t range (GeV/c)	Ξ^-/Λ	95% confidence interval
UA5	900	$\bar{p}p$	> 1	$0.07^{+0.08}_{-0.04}$	0.01–0.46
	546		> 1	0.6	0.26 (lower limits)
AFS	63	pp	1–2	0.06 ± 0.02	
TASSO	34.4	e^+e^-	all p_t	0.087 ± 0.042	
MARK II	29.0			0.08 ± 0.03	
HRS	29.0			0.073 ± 0.028	
TPC	29.0			0.101 ± 0.046	
CLEO	10.38–10.64			0.07 ± 0.01	
CLEO	$\Upsilon(1S)$			0.10 ± 0.02	
ARGUS	10.0			0.08 ± 0.01	

Also given are UA5 data at 546 GeV [2,3], pp data at 63 GeV and data from e^+e^- experiments (for references, see text). When both statistical and systematic errors have been given, they have been combined by adding their squares.

The 900 GeV result is consistent with the value of 0.06 ± 0.02 found at the ISR and ≈ 0.08 found in e^+e^- collisions. The high ratio of 0.6 (with a lower limit of 0.26 at 95% confidence level) measured at 546 GeV is probably due to an upward fluctuation in the Ξ^- yield.

We have also determined the Λ/K and Λ/n ratios in the region $|y| \leq 2$ using our data. More precisely, the ratios are $\langle n_\Lambda + n_{\bar{\Lambda}} + n_{\Sigma^0} + n_{\overline{\Sigma^0}} \rangle / 2 \langle n_{K^0_S} \rangle$ and $\langle n_\Lambda + n_{\bar{\Lambda}} + n_{\Sigma^0} + n_{\overline{\Sigma^0}} \rangle / 2 \langle n_{\bar{n}} \rangle$. The mean number of K^0_S has been measured in the range $|y| \leq 3.5$ [7] and the $\bar{n}$ rate has been determined in the region $|y| \leq 0.5$ [18]. The 546 GeV data on Λ's and K^0_S's are from ref. [3] and ref. [9], respectively. The mean number of antineutrons at 546 GeV is derived from UA2 data on protons [15] assuming $\sigma(n + \bar{n}) = \sigma(p + \bar{p})$ [3]. The particle yields were extrapolated or interpolated to the region $|y| \leq 2$ using the UA5 MC. We obtain a Λ/K ratio of 0.31 ± 0.09 at 200 GeV, 0.22 ± 0.05 at 546 GeV, and 0.26 ± 0.06 at 900 GeV. These values are consistent with those found in e^+e^- collisions, which are in the range 0.07–0.21 [25,27,28]. The Λ/n ratio is estimated to be 0.9 ± 0.5 at 200 GeV, 0.34 ± 0.08 at 546 GeV, and 0.8 ± 0.3 at 900 GeV. These ratios are compatible with the Λ/p value of 0.27 ± 0.02 measured at the ISR [23] and with the range of Λ/p values found in e^+e^- experiments, 0.16–0.39 [28,29].

3.5. SYSTEMATIC ERRORS

Three sources of systematic error have been studied: the extrapolation to zero of the fitted p_t function, the extrapolation from the limited rapidity region to full phase space, and the choice of y distribution in the acceptance calculation. The first

source clearly dominates the systematic error. For example, if one fits an exponential function of transverse mass $m_t = \sqrt{m^2 + p_t^2}$, instead of p_t, to our data the average transverse momenta increase and the particle yields decrease by about 20%. We therefore estimate the systematic error in $\langle p_t \rangle$ and in the hyperon rate per event to be 20%. The Ξ^-/Λ ratio is calculated in the limited range $p_t > 1$ GeV/c resulting in a smaller systematic error which is negligible compared to the statistical error.

4. Comparison with models

We have compared our results to the predictions of four particle production models. Three of them attempt to describe hadronic collisions in detail and have been implemented as Monte Carlo programs. They are the Dual Parton Model (DPM) [30, and references therein], the FRITIOF model [31], and the PYTHIA model [32]. Common to these models is the basic idea of string formation between quarks and/or diquarks in the colliding hadrons, followed by fragmentation of the strings into particles and resonances. The PYTHIA and FRITIOF models are based on the LUND fragmentation model [33]. In addition we have made comparisons with the Statistical Thermodynamical Model (STM) presented in ref. [34], which includes the formation of quark–gluon plasma.

To generate events according to the DPM model we have used a modified version [35] of the simulation program by Aurenche et al. [36]. This program has been tuned to describe the 546 GeV multiplicity distribution [3], the total pp ($\bar{p}p$) cross sections in the energy range 40–546 GeV [37, and references therein], and the $\nu p \to \pi^{\pm} X$ fragmentation functions [38].

For the PYTHIA MC program, the following non-default options were chosen. The option of variable impact parameters was selected, with a double gaussian distribution of matter in the incident hadrons. A smooth turnover between low-p_t soft gluon exchange processes and perturbative QCD was chosen, at an energy-dependent value. The turnover values used were 1.90 GeV/c at 200 GeV and 1.96 GeV/c at 546 and 900 GeV [39]. In the calculation of the strong coupling constant α_s, the option which takes into account a second-order evaluation was selected. In addition, several other non-default option values were used as recommended by the PYTHIA authors [39]. For the FRITIOF model the default parameters were used throughout but the program was modified to exclude single-diffractive events.

In the STM model it is assumed that all the available energy is transformed into a quark–gluon plasma with a temperature of 250 MeV and a radius of 3 fm. The plasma expands and cools until it reaches the critical temperature, 160 MeV, where the transition to the hadronic gas phase occurs. Since the total baryon number in $\bar{p}p$ collisions is zero we have used the model results valid at zero baryochemical potential [34]. The average transverse momenta were calculated using the thermal p_t distributions described in ref. [40], taking into account quantum statistics. A

TABLE 8
Model predictions compared to UA5 results

	Region	UA5	DPM	FRITIOF	PYTHIA	STM
$\sqrt{s} = 200$ GeV						
$\langle p_t \rangle_\Lambda$ (GeV/c)	$\|y\| \leq 2$	$0.80^{+0.20}_{-0.14}$	0.57	0.75	0.55	0.62
$\langle n_\Lambda \rangle$		0.27 ± 0.07	0.39	0.16	0.17	—
$\langle p_t \rangle_\Xi$ (GeV/c)	$\|y\| \leq 3$	$0.8^{+0.4}_{-0.2}$	0.61	0.74	0.57	0.66
$\langle n_{\Xi^-} \rangle$		$0.03^{+0.04}_{-0.02}$	0.04	0.02	0.02	—
Ξ^-/Λ	$\|y\| \leq 2$, $p_t > 1$ GeV/c	$0.10^{+0.13}_{-0.06}$	0.10	0.07	0.07	0.3–0.4
Λ/K	$\|y\| \leq 2$	0.31 ± 0.09	0.36	0.18	0.16	0.3–0.4
Λ/n	$\|y\| \leq 2$	0.9 ± 0.5	0.55	0.32	0.32	0.6–1.4
$\sqrt{s} = 546$ GeV						
$\langle p_t \rangle_\Lambda$ (GeV/c)	$\|y\| \leq 2$	0.62 ± 0.08	0.60	0.97	0.60	0.62
$\langle n_\Lambda \rangle$		0.25 ± 0.05	0.55	0.21	0.23	—
$\langle p_t \rangle_{\Xi^-}$ (GeV/c)	$\|y\| \leq 3$	1.1 ± 0.2	0.70	0.99	0.64	0.66
$\langle n_{\Xi^-} \rangle$		$0.08^{+0.03}_{-0.02}$	0.07	0.02	0.03	—
Ξ^-/Λ	$\|y\| \leq 2$, $p_t > 1$ GeV/c	0.6	0.10	0.08	0.08	0.3–0.4
Λ/K	$\|y\| \leq 2$	0.22 ± 0.05	0.38	0.18	0.17	0.3–0.4
Λ/n	$\|y\| \leq 2$	0.34 ± 0.08	0.55	0.30	0.33	0.6–1.4
$\sqrt{s} = 900$ GeV						
$\langle p_t \rangle_\Lambda$ (GeV/c)	$\|y\| \leq 2$	0.74 ± 0.09	0.62	1.08	0.64	0.62
$\langle n_\Lambda \rangle$		0.38 ± 0.08	0.64	0.24	0.26	—
$\langle p_t \rangle_\Xi$ (GeV/c)	$\|y\| \leq 3$	$0.7^{+0.2}_{-0.1}$	0.70	1.4	0.73	0.66
$\langle n_{\Xi^-} \rangle$		$0.05^{+0.04}_{-0.02}$	0.08	0.03	0.03	—
Ξ^-/Λ	$\|y\| \leq 2$, $p_t > 1$ GeV/c	$0.07^{+0.08}_{-0.04}$	0.09	0.08	0.07	0.3–0.4
Λ/K	$\|y\| \leq 2$	0.26 ± 0.06	0.39	0.18	0.18	0.3–0.4
Λ/n	$\|y\| \leq 2$	0.8 ± 0.3	0.58	0.30	0.33	0.6–1.4

The particle yields are given per non-single-diffractive event. The ratios are explained in the text. The lower and upper limits given for the ratios predicted by the STM model correspond to slow and fast volume expansion of the quark–gluon plasma, respectively.

hadronization temperature of 160 MeV was assumed, as above, and particle emission at higher temperatures was ignored.

The results are shown in table 8. The agreement is good except for the average p_t of Λ's where the FRITIOF model predictions at 546 and 900 GeV are too high and the Λ yields where the DPM model predicts too high values at 546 and 900 GeV. The high value of the Ξ^-/Λ ratio found by UA5 at 546 GeV was interpreted as a

possible sign of quark–gluon plasma [41]. The lower 900 GeV value is in good agreement with data from other experiments but it does not rule out even the extreme case of all particle production in every $\bar{p}p$ interaction occurring via the quark–gluon plasma.

5. Conclusions

Results have been presented on the production of Λ and Ξ^- hyperons in $p\bar{p}$ collisions at 200 and 900 GeV. The data samples are based on decays seen in the UA5 streamer chambers. The following conclusions can be drawn from the data:

(i) The p_t distributions of Λ's are well described by an exponential function in p_t. We find an average transverse momentum of $0.80^{+0.20}_{-0.14}$ GeV/c at 200 GeV and 0.74 ± 0.09 GeV/c at 900 GeV in the rapidity region $|y| \leqslant 2$. The average p_t of Ξ^-'s in the range $|y| \leqslant 3$ is estimated to be $0.8^{+0.4}_{-0.2}$ GeV/c at 200 GeV and $0.7^{+0.2}_{-0.1}$ GeV/c at 900 GeV. Our best estimate of the Ξ^- average momentum at the highest Collider energies is the fit to the combined 546 and 900 GeV samples which gives a value of 0.9 ± 0.1 GeV/c. The Λ and Ξ^- $\langle p_t \rangle$'s are consistent with being equal and seem to be slightly higher than the $\langle p_t \rangle$ found for K^0_S's at the same energies. Taking all the baryon production together it appears that the $\langle p_t \rangle$ has increased in going from the ISR to the Collider.

(ii) The Λ yield has increased significantly when going from lower energies to the Collider energy range. The energy evolution of the Λ rate is similar to that of the total charged multiplicity and is well described by a second degree polynomial in $\ln s$. The mean number of Λ's per inelastic event is estimated to be 0.42 ± 0.11 at 200 GeV and 0.66 ± 0.14 at 900 GeV. The Ξ^- yield per inelastic event is found to be $0.03^{+0.04}_{-0.02}$ at 200 GeV and $0.06^{+0.05}_{-0.03}$ at 900 GeV. The Ξ^- corrected rates at 546 and 900 GeV are very close in spite of the large difference in the observed rates. This is due to the sensitivity of the correction procedure to the $\langle p_t \rangle$ which differs between the two energies. Assuming the yields and $\langle p_t \rangle$'s to be the same at the two energies, a simple calculation shows that the results are compatible at the 1% level.

(iii) The ratio of Ξ^- to Λ production obtained at 900 GeV in the region $p_t > 1$ GeV/c is $0.07^{+0.08}_{-0.04}$, which is consistent with the ratios found in e^+e^- collisions and in pp collisions at 63 GeV c.m. energy. The surprisingly high value of 0.6 measured at 546 GeV appears to be an upward fluctuation when compared to the new data. Our upper limit at 95% confidence level is 0.46 at 900 GeV.

(iv) The Dual Parton, FRITIOF, and PYTHIA models describe most of the data well. Exceptions are the high average p_t's of Λ's predicted by the FRITIOF model at 546 and 900 GeV and the high mean number of Λ's given by the DPM model at 546 and 900 GeV and the high mean number of Λ's given by the DPM model at 546 and 900 GeV. The enhancement of strange particle production predicted by the Statistical Thermodynamical Model to result from the formation of quark–gluon plasma cannot be ruled out on the basis of our data.

We would like to express our gratitude to the CERN staff for the excellent way the pulsed collider mode was set up and run. We acknowledge with thanks the financial support of the Brussels group by the National Foundation for Fundamental Research and the Inter-University Institute of Nuclear Sciences, of the Bonn group by the Bundesministerium für Wissenschaft und Forschung, of the Cambridge group by the Science and Engineering Research Council, and of the Stockholm group by the Swedish Natural Science Research Council. Last but not least, we acknowledge the contribution of the engineers, scanning and measuring staff of all our laboratories.

References

[1] M. Jacob and J. Rafelski, Phys. Lett. B190 (1987) 173
[2] UA5 Coll., G.J. Alner et al., Phys. Lett. B151 (1985) 309
[3] UA5 Coll., G.J. Alner et al., Phys. Rep. 154 (1987) 247
[4] J.G. Rushbrooke, Proposal for achieving $p\bar{p}$ collisions at up to 1 TeV c.m. energy by means of a cyclic variation of stored beam energy in the SPS Collider. CERN/EP/82-6 (1982);
UA5 Coll.: An exploratory investigation of $p\bar{p}$ interactions at 800–900 GeV c.m. energy at the SPS Collider, UA5/2 Proposal CERN/SPSC/82-75/P184 (1982)
[5] UA5 Coll., G.J. Alner et al., Z. Phys. C32 (1986) 153
[6] UA5 Coll., R.E. Ansorge et al., Z. Phys. C33 (1986) 175
[7] UA5 Coll., R.E. Ansorge et al., Z. Phys. C41 (1988) 179
[8] K. Jon-And and Ch. Walck, Treatment of strange particle decays observed in the UA5 streamer chambers, Univ. of Stockholm report USIP 85-16 1985
[9] UA5 Coll., G.J. Alner et al., Nucl. Phys. B258 (1985) 505
[10] UA5 Coll., R.E. Ansorge et al., Charged particle multiplicity distributions at 200 and 900 GeV c.m. energy, CERN-EP/88-172 (1988) Z. Phys. C, to be published
[11] UA5 Coll., K. Alpgård et al., Phys. Lett. B115 (1982) 65
[12] UA5 Coll., G.J. Alner et al., Nucl. Phys. B291 (1987) 445
[13] 69 GeV/c: V.V. Ammosov et al., Nucl. Phys. B115 (1976) 269;
300 GeV/c: F. LoPinto et al., Phys. Rev. D22 (1980) 573;
E735 Coll., S. Banerjee et al., Phys. Rev. Lett. 62 (1989) 12
[14] A.M. Rossi et al., Nucl. Phys. B84 (1975) 269
[15] UA2 Coll., M. Banner et al., Phys. Lett. B122 (1983) 322
[16] UA1 Coll., G. Arnison et al., Phys. Lett. B118 (1982) 167;
F. Ceradini (UA1 Coll.); Proc. Int. Europhysics Conf. on High Energy physics, Bari, Italy, 1985, ed. L. Nitti and G. Preparata (European Physical Society, Geneva, 1985), p. 363;
CDF Coll., F. Abe et al., Phys. Rev. Lett. 61 (1988) 1819;
T. Alexopoulos et al., Phys. Rev. Lett. 60 (1988) 1622
[17] UA5 Coll., G.J. Alner et al., Phys. Lett. B167 (1986) 476
[18] L. Burow, Untersuchungen zur Baryonproduktion in Proton–Antiproton-Wechselwirkungen bei Schwerpunktsenergien von 200 bis 900 GeV, PhD Thesis, Univ. of Bonn report BONN-IR-87-25 1987;
R.S. De Wolf, Charged and neutral particle production in $\bar{p}p$ interactions at 200 and 900 GeV c.m. energies, PhD Thesis, Univ. of Cambridge (1986)
[19] 24 GeV/c: V. Blobel et al., Nucl. Phys. B69 (1974) 454
[20] 100 GeV/c: M. Alston-Garnjost et al., Phys. Rev. Lett. 35 (1975) 142;
102 GeV/c: J.W. Chapman et al., Phys. Lett. B47 (1973) 465;
147 GeV/c: D. Brick et al., Nucl. Phys. B164 (1980) 1;
205 GeV/c: K. Jaeger et al., Phys. Rev. D11 (1975) 2405;
300 GeV/c: A. Sheng et al., Phys. Rev. D11 (1975) 1733;

303 GeV/c: F.T. Dao et al., Phys. Rev. Lett. 30 (1973) 1151;
360 GeV/c: M. Asai et al., Z. Phys. C27 (1985) 11;
400 GeV/c: R.D. Kass et al., Phys. Rev. D20 (1979) 605;
405 GeV/c: H. Kichimi et al., Phys. Rev. D20 (1979) 37
[21] UA5 Coll., G.J. Alner et al., Z. Phys. C33 (1986) 1
[22] UA5 Coll., R.E. Ansorge et al., Z. Phys. C, submitted
[23] AFS Coll., T. Åkesson et al., Nucl. Phys. B246 (1984) 1
[24] ARGUS Coll., H. Albrecht et al., Phys. Lett. B183 (1987) 419
[25] CLEO Coll., M.S. Alam et al., Phys. Rev. Lett. 53 (1984) 24
[26] HRS Coll., S. Abachi et al., Phys. Rev. Lett. 58 (1987) 2627;
H. Yamamoto (TPC Coll.), Proc. Hadronic session of the twentieth Rencontre de Moriond, ed. J. Tran Thanh Van (Editions Frontières, Paris, 1985);
MARK II Coll., S.R. Klein et al., Phys. Rev. Lett. 58 (1987) 644;
TASSO Coll., M. Althoff et al., Phys. Lett. B130 (1983) 340
[27] HRS Coll., M. Derrick et al., Phys. Rev. D35 (1987) 2639
[28] TASSO Coll., M. Althoff et al., Z. Phys. C27 (1985) 27
[29] CLEO Coll., S. Behrends et al., Phys. Rev. D31 (1985) 2161
[30] A. Capella and J. Tran Thanh Van, Z. Phys. C23 (1984) 165
[31] B. Andersson, G. Gustafson and B. Nilsson-Almqvist, Nucl. Phys. B281 (1987) 289;
B. Nilsson-Almqvist and E. Stenlund, Comp. Phys. Commun. 43 (1987) 387;
B. Andersson, G. Gustafson and B. Nilsson-Almqvist, A high energy string dynamics model for hadronic interactions, Lund preprint LU TP 87-6 (1987)
[32] H.U. Bengtsson and T. Sjöstrand, Comp. Phys. Commun. 46 (1987) 43;
T. Sjöstrand and M. van Zijl, Phys. Rev. D36 (1987) 2019
[33] B. Andersson et al., Phys. Rep. 97 (1983) 33
[34] P. Koch, B. Müller and J. Rafelski, Phys. Rep. 142 (1986) 167
[35] B. Holl, Die Production geladener Hadronen in Proton-Antiproton-Wechselwirkungen bei Schwerpunktsenergien von 200 bis 900 GeV im Vergleich zu den Vorhersagen des Dual-Parton-Modells, BONN-IR-86-15 (1986)
[36] P. Aurenche, F.W. Bopp and J. Ranft, Z. Phys. C23 (1984) 67;
F.W. Bopp, P. Aurenche and J. Ranft, Phys. Rev. D33 (1986) 1876
[37] N. Amos et al., Nucl. Phys. B262 (1985) 689;
UA4 Coll., M. Bozzo et al., Phys. Lett. B147 (1984) 392
[38] Aachen–Bonn–CERN–München(MPI)–Oxford Coll., P. Allen et al., MPI-PAE/EXP.EL.106 (1982)
[39] T. Sjöstrand, private communication
[40] R. Hagedorn, Riv. Nuovo Cimento 6 (1983) No. 10
[41] J. Rafelski, Proc. 22nd Rencontre de Moriond, ed. J. Tran Thanh Van (Editions Frontières, Paris, 1987)